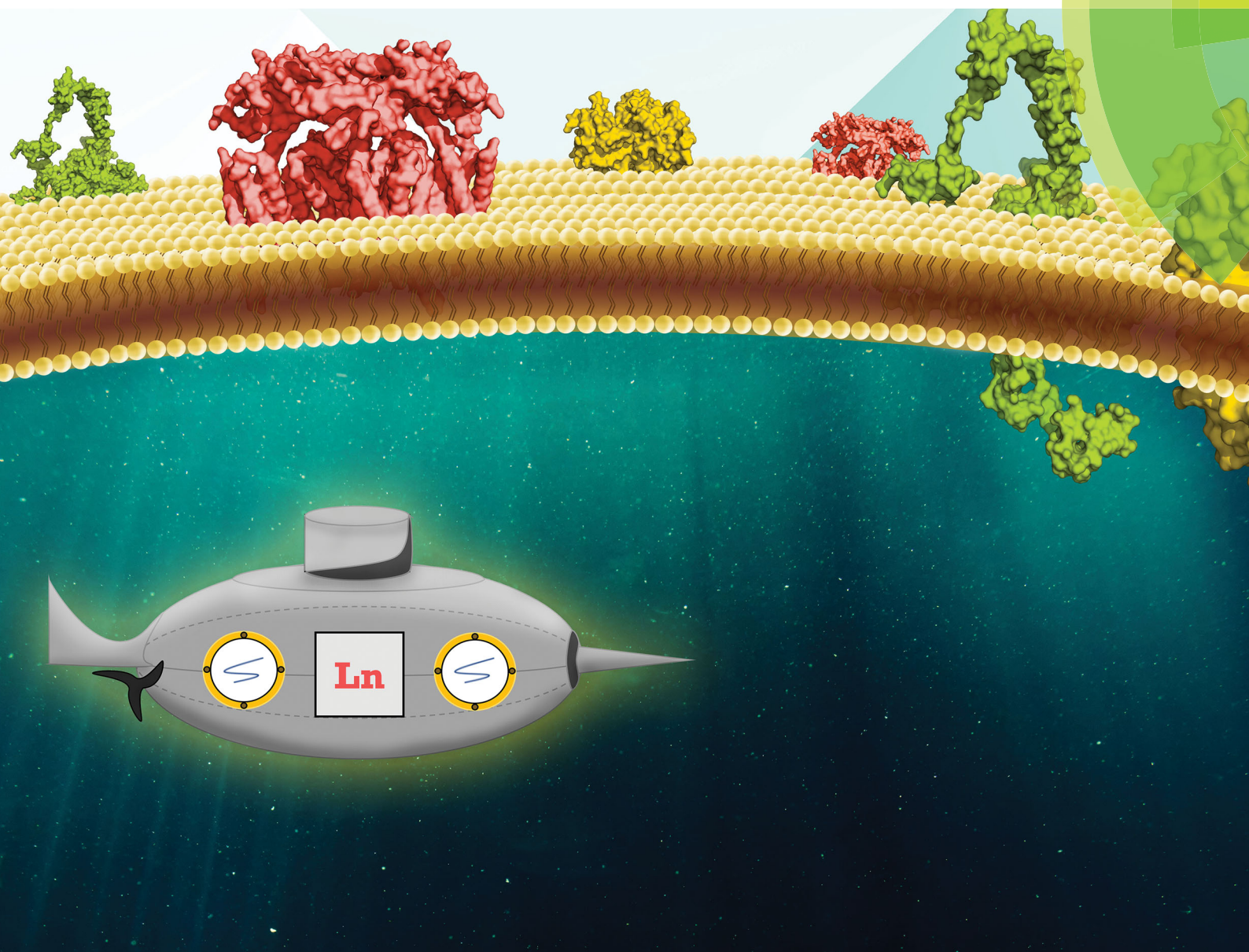


# ChemComm

Chemical Communications

[rsc.li/chemcomm](http://rsc.li/chemcomm)



ISSN 1359-7345



FEATURE ARTICLE

K. Eszter Borbas *et al.*

Lanthanide-based tools for the investigation of cellular environments



Cite this: *Chem. Commun.*, 2018, 54, 10021

# Lanthanide-based tools for the investigation of cellular environments

Emilie Mathieu, Agnès Sipos,  † Ellen Demeyere, ‡ Dulcie Phipps, § Dimitra Sakaveli ¶ and K. Eszter Borbas  \*

Biological probes constructed from lanthanides can provide a variety of readout signals, such as the luminescence of Eu(III), Tb(III), Yb(III), Sm(III) and Dy(III), and the proton relaxation enhancement of Gd(III) and Eu(II). For numerous applications the intracellular delivery of the lanthanide probe is essential. Here, we review the methods for the intracellular delivery of non-targeted complexes (*i.e.* where the overall complex structure enhances cellular uptake), as well as complexes attached to a targeting unit (*i.e.* to a peptide or a small molecule) that facilitates delivery. The cellular applications of lanthanide-based supramolecules (dendrimers, metal organic frameworks) are covered briefly. Throughout, we emphasize the techniques that can confirm the intracellular localization of the lanthanides and those that enable the determination of the fate of the probes once inside the cell. Finally, we highlight methods that have not yet been applied in the context of lanthanide-based probes, but have been successful in the intracellular delivery of other metal-based probes.

Received 1st July 2018,  
Accepted 30th July 2018

DOI: 10.1039/c8cc05271a

rsc.li/chemcomm

## Introduction

Probes based on lanthanide(III) ions are ubiquitous in the life sciences. The luminescence of Eu (red) and Tb (green), and, increasingly, Sm (orange), Dy (yellow), Yb and Nd (both near infrared; NIR) makes them excellent tools for spectroscopy or microscopy. Highly paramagnetic Gd(III) with its 7 unpaired electrons and isoelectronic Eu(II) are used as MRI contrast agents,<sup>1–6</sup> although Eu(II) has interesting, and so far little explored photophysics.<sup>7–10</sup>

Department of Chemistry, Ångström Laboratory, Uppsala University, Box 523, 75120, Uppsala, Sweden. E-mail: eszter.borbas@kemi.uu.se

† Exchange MSc student from Département de chimie, École normale supérieure, PSL University, 75005 Paris, France

‡ Exchange BSc student from the Ghent University, Belgium

§ Erasmus student from the University of Glasgow, Scotland

¶ Erasmus student from the University of Crete, Greece



Emilie Mathieu

*Emilie Mathieu was born in Echirolles, France. She obtained her MSc in Chemistry in 2014 (Sorbonne University and the Ecole Normale Supérieure, Paris, France); she worked on the synthesis of gentiopicroside (Prof. Serge Thorimbert, Dr Luc Dechoux). She then worked on the role of copper in Alzheimer's disease (Prof. Tim Storr, Vancouver, Canada). During her PhD, which she obtained in September 2017, she studied*

*manganese complex superoxide dismutase mimics and their cellular behavior under the supervision of Prof. Clotilde Policar and Dr Nicolas Delsuc. She is currently a postdoctoral fellow at Uppsala University, working on lanthanide coordination chemistry.*



Agnès Sipos

*Agnès Sipos was born in Meudon (France) in 1996. She obtained her BSc degree in 2017 from the Ecole Normale Supérieure in Paris after an internship in Christelle Hureau's group in Toulouse, where she did research on metal in a sperm peptide. She joined the Borbas group for an internship during her 1st year of master's. She is interested in inorganic chemistry and its applications to biology. She is preparing for the competitive teachers' examination before finishing her master's degree.*



Lanthanide luminescence is due to 4f–4f transitions. The f-electrons are buried and do not participate in bonding interactions with the ligand. Therefore, crystal field effects are small, and absorption and emission bands are sharp.<sup>11</sup> The emission spectra of the lanthanide ions most often used in cellular imaging are shown in Fig. 1. The f–f transitions are forbidden by the Laporte selection rule, which can be relaxed by vibronic coupling or mixing with other orbitals. As a consequence, lanthanides have very weak molar extinction coefficients ( $\sim 1 \text{ L mol}^{-1} \text{ cm}^{-1}$ ),<sup>12</sup> which implies that direct excitation of the  $\text{Ln}^{3+}$  ion will lead to very weak emission. This limitation is overcome by using a light-harvesting ‘antenna’, i.e. photosensitizer in the close vicinity of the metal ion, usually coupled to the ligand. Upon excitation, the antenna transfers its energy to the excited state of the  $\text{Ln}^{3+}$  ion, which can subsequently emit light (Fig. 1). The rate constant of the energy transfer between the antenna and the lanthanide ion is much higher compared to the luminescence emission lifetime of the

lanthanide ( $k_{\text{ET}} \gg k_{\text{lum}}$ ).<sup>13</sup> The efficiency of the energy transfer is dependent on the difference between the energy levels of the excited states of the ligand and the lanthanide. Quenching mechanisms include back energy transfer (BET, most often for Tb), photo-induced electron transfer (PeT, for the more reducible lanthanide(III) ions<sup>14,15</sup>), or coupling to X–H oscillators (X = O, N, C).<sup>16,17</sup> Lanthanide emitter design has been covered in several recent reviews.<sup>18,19</sup>

Lanthanide luminescence is characterized by long lifetimes ( $\mu\text{s}$  (Yb, Nd) to ms (Eu, Tb)) compared to that of organic fluorophores (ns).<sup>20</sup> Large pseudo-Stokes shifts are observed, because the excitation wavelength of the antenna is usually in the 320–400 nm range, while that of the lanthanide emission is between 500 and 1500 nm. This makes lanthanide emitters less prone to auto-quenching. Furthermore, these complexes are more photostable than organic fluorophores.

Lanthanide luminescence is tailor-made for multiplex imaging. This includes not just the simultaneous detection of



**Ellen Demeyere**

*Ellen Demeyere was born in 1997 in Ghent, Belgium. She earned her BSc in chemistry in 2018 from Ghent University after having completed an Erasmus exchange at Uppsala University, Sweden, where she worked in the research group of Eszter Borbas on the design and synthesis of luminescent lanthanide complexes. She will start her MSc studies in chemistry at Ghent University in the fall of 2018 with focus on organic chemistry.*



**Dulcie Phipps**

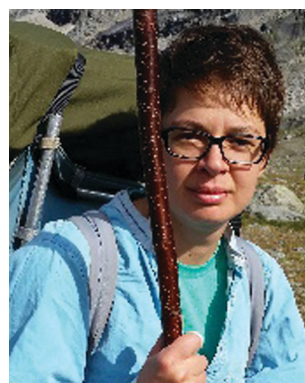
*Dulcie Phipps was born in Birmingham, England, but moved to Scotland when she was two years old and has lived there all her life. She is an undergraduate student at the University of Glasgow, with interest in nanoscience and in particular coordination chemistry. After graduating from her final year in 2019, Dulcie plans to find a PhD outside of the UK.*



**Dimitra Sakaveli**

*Dimitra Sakaveli was born in Heraklion of Crete, Greece. Dimitra completed her BSc in 2017 at the Department of Chemistry at the University of Crete, after completing an undergraduate thesis in the Laboratory of Bioinorganic Chemistry under the supervision of Professor A. Coutsolelos. In 2018 she worked in the Borbas lab at Uppsala University as part of a three month Erasmus+ internship. She is interested in materials*

*chemistry and medical applications. Next year she will start an MSc in the Medical School at the University of Crete.*



**K. Eszter Borbas**

*Eszter Borbas grew up in Hungary and in Yemen. After completing her undergraduate studies at Eötvös University in Budapest with research work in József Rábai's group, she did her PhD at the Open University (with James Bruce), and she was a postdoc at North Carolina State University (with Jonathan Lindsey), and a Marie Curie fellow at Stockholm University in Sweden. She started her independent career in 2010 as a Swedish Research Council assistant professor. She is currently an associate professor at Uppsala University, where her research group works on lanthanide chemistry and photophysics, and on tetrapyrrole chemistry.*



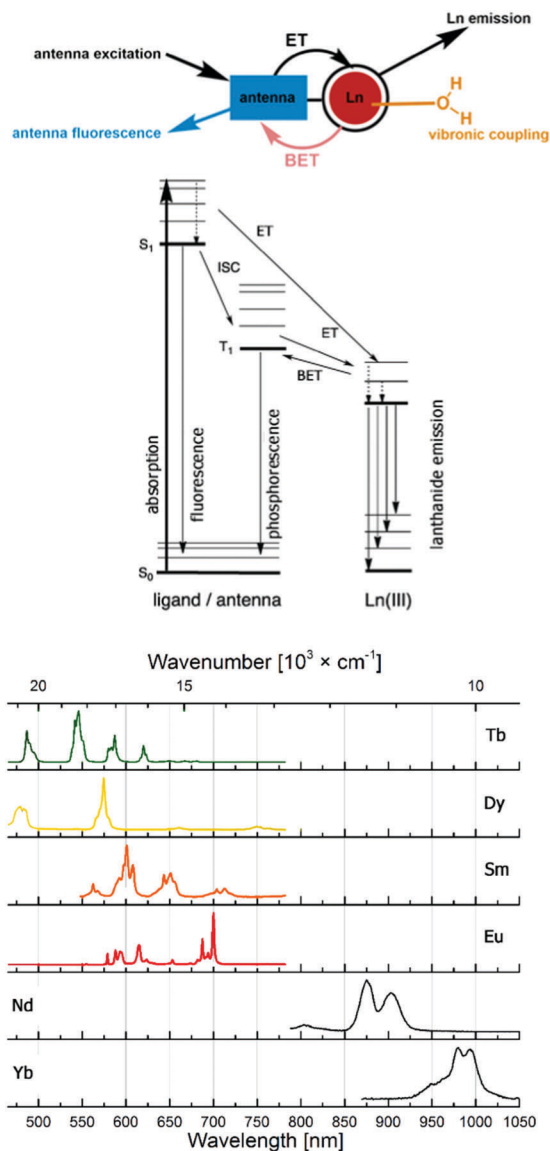


Fig. 1 Antenna effect, with major deactivation pathways shown in colour, and productive pathways for lanthanide sensitization in black (top). Emission spectra of the most commonly used lanthanide(III) emitters (bottom).

luminescent tags, but also the real-time monitoring of dynamic processes, and the measurements of analytes with changing concentrations, enzymes with changing activities, *etc.* One of the most challenging environments for doing this is in live cells, and not surprisingly, the dynamic multiplex detection of interacting analytes in living cells is not yet within reach. In order to achieve this goal, at least three things need to be optimized. (1) The design of the responsive probes needs to be optimized. These probes must of course be selective for their targets, have a large dynamic range, high water solubility and photostability, and low toxicity. Ideally, their design should be modular, and their synthesis short, convergent, and scalable.<sup>21</sup> (2) The photophysical properties of the complexes need to be optimized. This comprises high quantum yields, which in turn necessitates the understanding of quenching pathways.<sup>14</sup>

(3) The probes must be able to enter target cells, and must be able to detect their target analytes.

Here, we will focus on the third aspect of probe design. We will present current strategies for delivering a lanthanide payload into cells, with an additional focus on the techniques that can confirm the internalization and the cellular localization of the metals. While we will focus on luminescent lanthanides, where appropriate, Gd(III) MRI contrast agents will be discussed. We will also briefly look at methods to target lanthanide complexes to the outside cell membranes. There are a number of relatively recent reviews on areas that partially overlap with the current topic: luminescent lanthanide labels in microscopy,<sup>22</sup> lanthanide probes for detecting protein–protein interactions,<sup>23</sup> responsive Eu-based probes,<sup>24</sup> and the design of targeting extracellular receptors.<sup>25</sup>

## Imaging techniques

The luminescent properties of lanthanide complexes are highly valuable to study their mechanism(s) of internalization in living cells. Cell penetration of these complexes can be followed in real time in living cells and give insight into uptake pathways and kinetics.<sup>26</sup> Their long emission lifetimes limit signal contamination by endogenous chromophores (*e.g.* NAD(P)H, flavine, Trp, Tyr) that have nanosecond lifetimes.<sup>20</sup>

Imaging techniques that take advantage of the photo-physical properties of the lanthanides have been developed. Time-resolved fluorescence microscopy has been optimized to match the requirements of short and intense excitation pulses, tuneable delay times, and tuneable detection windows (Fig. 2).<sup>13,27–29</sup> The introduction of a delay between an excitation pulse and the detection of the emission (10–200  $\mu$ s) yields a luminescence signal free from the fluorescent background, which improves the signal-to-noise ratio.

Multi-photon absorption microscopy is suitable for the study of lanthanide complexes. The wavelength used to excite the antenna (320–400 nm) can lead to photo-damage in cells. Two- and three-photon<sup>30</sup> excitation spectroscopies use excitation wavelengths in the far visible/near-IR range (700–900 nm).<sup>31–34</sup> Further developments have extended this method to NIR emitters (Yb, Nd).<sup>31–33</sup> This technique can be used to follow

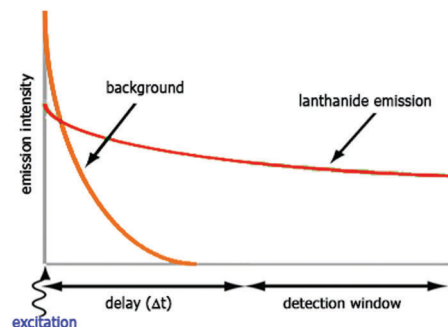
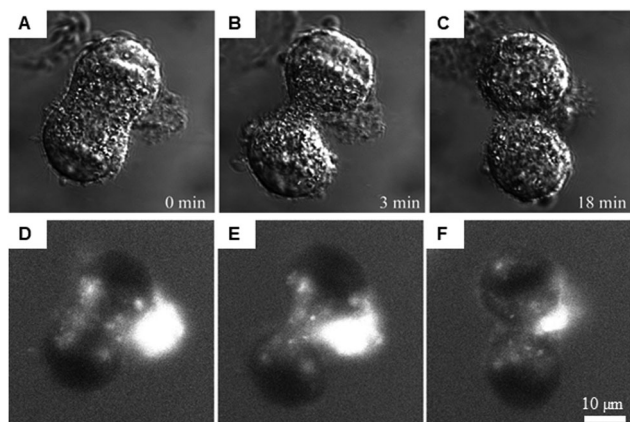


Fig. 2 Time-resolved luminescence measurements. The sample is irradiated with a pulse at the excitation wavelength, and the emission intensity is recorded after a delay time ( $\Delta t$ ) for a defined period (detection window).





**Fig. 3** Intracellular distribution of  $[\text{Na}_3][\text{EuL}^1\text{G}^3]$  in live cells after mild saponin permeabilization. Adapted from ref. 34 with permission from the Royal Society of Chemistry. A mitotic cell 24 h after treatment is shown, and dye solution was added to the culture medium after saponin was rinsed out. Transmitted light DIC images of different stages of mitosis (A–C) and the corresponding  $[\text{Na}_3][\text{EuL}^1\text{G}^3]$  2P luminescence images (D–F).

the distribution of luminescent europium complexes in living T24 human cancer cells during mitosis as displayed in Fig. 3.<sup>34</sup>

Finally, lifetime imaging microscopy enables mapping of emission lifetimes in cells, which gives useful information on the environment of the complex. In short, the intensity decay in each pixel is fit by an exponential (or a multi-exponential) decay. The emission lifetime ( $\tau$ ) value for each pixel is extracted and a map showing the different  $\tau$  values is constructed.<sup>13,20,32–34</sup> Changes in emission lifetimes can give indications on  $\text{O}_2$  concentration in cells,<sup>35–37</sup> colocalization with a FRET (Förster resonance energy transfer) acceptor,<sup>34</sup> and changes in polarity, viscosity or lipophilicity.<sup>38</sup>

## Mechanisms governing cell penetration

The subcellular localization of lanthanide complexes depends primarily on the mechanism(s) by which they are taken up by the cell. A combination of luminescence microscopy and the use of inhibitors or promoters of known uptake pathways has been used to better understand how the complexes are internalized in cells, and is presented in the following. Uptake pathways depend on the type of cell, and the size, charge and lipophilicity of the compounds. The cellular uptake mechanism(s) of non-functionalized lanthanide complexes is first described and followed by the modifications that have been made to lanthanide complexes to enhance or limit their cell penetration, as well as to direct them to subcellular compartments.

### Passive diffusion

The different uptake pathways are depicted in Fig. 4.<sup>26,39,40</sup> The existence of a concentration gradient between the extracellular media and the cell can lead to a passive diffusion of complexes inside the cell.<sup>26</sup> Measurements of cell penetration at low temperature (4–5 °C) help discriminate between passive and

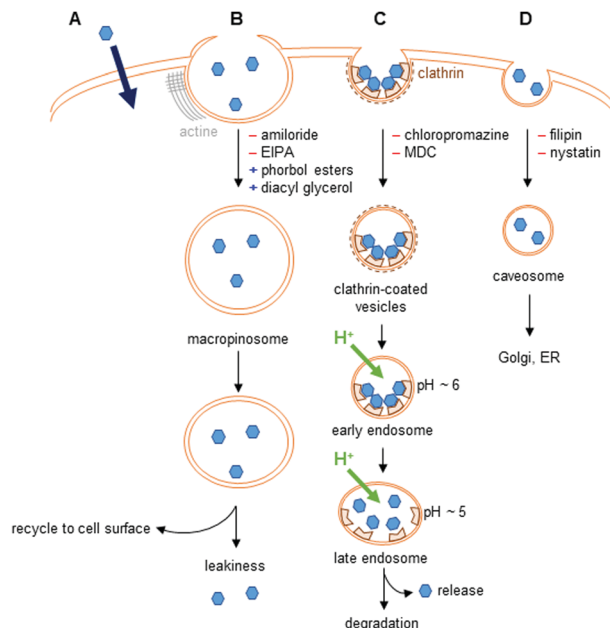


**Fig. 4** Uptake pathways in cells. (A) Passive diffusion. (B) Macropinocytosis. Amiloride and 5-(*N*-ethyl-*N*-isopropyl)amiloride (EIPA) are inhibitors of this pathway, whereas phorbol esters and diacyl glycerol promote it. (C) Clathrin-mediated endocytosis. Interaction with receptors at the cell surface leads to the formation of clathrin-coated vesicles. This pathway is inhibited by chlorpromazine, or monodansylcadaverine (MDC); however, these two inhibitors also disturb macropinocytosis. (D) Caveolin-dependent endocytosis. This pathway is inhibited by filipin and nystatin.

active internalization of compounds, but low temperature measurements imply the underestimation of the contribution of the translocation mechanism.<sup>41</sup> Metabolic inhibitors can also give insights into the type of mechanism involved. The use of sodium azide,<sup>42</sup> iodoacetate,<sup>42,43</sup> or 2-deoxyglucose<sup>26</sup> has been described in the literature. Indeed, active pathways are energy-dependent and are thus inhibited when working at low temperature.

### Endocytosis

The endocytic pathways proceed through an invagination of the cell membrane that is energy-dependent, and lead to the internalization of macromolecules or solutes. There are two endocytic categories, phagocytosis, which occurs in macrophages, and pinocytosis, which is common to all cell types. Four pathways of pinocytosis are usually acknowledged: macropinocytosis, clathrin-mediated endocytosis, caveolin-mediated endocytosis, and clathrin/caveola-independent endocytosis.<sup>26,39,40</sup>

Macropinocytosis corresponds to the actin-dependent formation of a cup-shaped ruffle at the cell surface, which closes to form a macropinosome.<sup>39</sup> This vesicle is large, and complexes can leak into the cell. The macropinosome is then recycled to the cell surface. This pathway does not involve interaction with receptors.

In clathrin-mediated endocytosis, interaction of the complex with receptors at the surface of the cell leads to the formation of clathrin-coated vesicles.<sup>39</sup> These vesicles mature into early,



then late endosomes, before fusing with lysosomes, leading to the degradation of their content. During the maturation, the pH of the vesicles drops to  $\sim 5$ . Endosomal release to lysosomes, the Golgi apparatus, or the nucleus has been observed. The content of endosomes can also be recycled to the cell surface.

Caveolin-dependent endocytosis is a small invagination of the cell membrane that leads to the formation of caveosomes in cells. These caveosomes are usually directed to the Golgi apparatus or to the endoplasmic reticulum (ER). This mechanism is involved in the uptake of, *e.g.*, folic acid. Caveolin-dependent endocytosis was first described as an uptake mechanism that does not lead to lysosomal degradation, but this is now questioned as some evidence indicates that the vesicles formed fuse with lysosomes.<sup>40</sup>

Other uptake pathways that are mediated by interactions with receptors at the cell surface and are clathrin- and caveola-independent have also been described.

Different inhibitors and promoters can help investigate the mechanism(s) of cell penetration of lanthanide complexes, even though they are usually not specific inhibitors of one given pathway.<sup>26,39,40</sup> Because these compounds interfere with cellular homeostasis, they can show non-specific toxicity and should be used with caution.<sup>26,40</sup> Amiloride and its derivatives are known inhibitors of macropinocytosis that impact  $\text{Na}^+/\text{H}^+$  exchange at the cell membrane and decrease the submembranous pH, whereas phorbol esters and diacyl glycerol promote macropinocytosis. Among the other inhibitors described in the literature, wortmannin is frequently used. However, this inhibitor is not specific, and can also inhibit clathrin- and caveolin-mediated endocytosis. Clathrin-mediated endocytosis is inhibited by chlorpromazine, monodansylcadaverine (MDC) and dynasore. However, these inhibitors can impact other endocytic pathways: the first two inhibiting macropinocytosis, while dynasore acts on caveolin-mediated endocytosis.  $\text{K}^+$  depletion or the use of a hypertonic medium enriched with sucrose also inhibits clathrin-mediated endocytosis. These methods are non-selective, and can perturb several endocytic pathways, as well as cellular physiology. Finally, inhibitors of caveolin-dependent endocytosis include filipin and nystatin, with pronounced toxicity.<sup>40</sup>

Colocalization with stains specific for endosomes or lysosomes can be used to obtain further information on the uptake mechanism(s).<sup>26,40</sup> Co-incubation with fluorescently labelled low-density lipoproteins (LDLs) or transferrin enables clathrin-mediated endocytosis.

For cell-impermeable lanthanides, techniques, such as micro-injection,<sup>27,44</sup> reversible plasma membrane permeabilization,<sup>45</sup> and osmotic lysis of pinocytic vesicles,<sup>29,45</sup> have been used. Co-incubation with compounds that increase cell permeability such as DMSO,<sup>30,46,47</sup> saponin,<sup>34</sup> or TMPyP<sup>48</sup> has also been described.

### Quantification of uptake

Ln complexes are usually detected by luminescence methods, which, however, do not give quantitative information on the

amount of complex internalized. Luminescence emission can be quenched by endogenous electron-rich molecules (urate, ascorbate, citrate, ATP, phosphate, lactate) through electron or charge transfer quenching.<sup>49,50–55</sup> Interaction with proteins, DNA or RNA decreases the overall emission intensity.<sup>50,53,55,56</sup> Other molecules such as promoters or inhibitors used to study lanthanide internalization can also quench the luminescence emission.<sup>57</sup> Self-quenching due to aggregation has been reported.<sup>57</sup> Thus, alternative methods providing quantitative information on the accumulation of Ln complexes should be used, such as inductively-coupled plasma mass spectrometry (ICP-MS), or atomic absorption spectroscopy (AAS).<sup>26,58</sup>

### Stability of Ln complexes in cells

A final factor to consider is the inertness and stability of lanthanide complexes in cells. Careful analysis of the excitation and emission spectra of the lanthanides (especially those of Eu species) in cells as well as their emission lifetimes can help determine the integrity of the emitter. In some cases, evidence of interactions with endogenous species, *e.g.* proteins, can be obtained.

### Helicates

Bünzli and coworkers studied emissive bimetallic lanthanide complexes with helical structures in cells.<sup>59</sup> The uptake mechanism of  $[\text{Eu}_2(\text{LC}^2)_3]$  in HeLa cells was studied in depth.<sup>60,61</sup> Time-resolved microscopy was used to follow the internalization of the complex. Lanthanide luminescence was observed from inside the cells after 15 min incubation. The uptake of  $[\text{Eu}_2(\text{LC}^2)_3]$  was decreased at 4 °C, demonstrating that the uptake proceeds through an active mechanism.<sup>61</sup> The accumulation of the complex was determined in the presence of sodium azide (inhibitor of cellular respiration), sodium iodoacetate (inhibitor of anaerobic glycolysis), a hypertonic sucrose treatment (inhibitor of clathrin-dependent endocytosis), or potassium depletion (inhibitor of clathrin-dependent endocytosis).<sup>60</sup> The first two treatments lead to a decrease in ATP production.<sup>42,43</sup> A lower uptake of the complex following these two treatments was observed, which suggests that  $[\text{Eu}_2(\text{LC}^2)_3]$  is taken up in cells through an active pathway. In addition, the uptake of  $[\text{Eu}_2(\text{LC}^2)_3]$  decreased when cells were treated with sucrose, or when potassium is depleted from the cell culture medium. These observations additionally suggest that the complex enters the cells through an endocytic pathway. However, a change in cell morphology can be observed for  $\text{K}^+$  depletion treatment, and to a lesser extent for hypertonic treatment. An important message here is that cell pathway inhibitors and promoters should be used with caution to avoid the non-specific toxicity and perturbation of cell homeostasis.<sup>39</sup> Interestingly, co-staining experiments with BIODIPY FL labeled low density lipoprotein (LDL) or transferrin were run.<sup>61</sup> LDL and transferrin uptake followed a clathrin-mediated endocytosis. LDL interacts with the LDL receptor at the cell surface, which leads to the formation of clathrin-coated vesicles (CCV), which are released from late endosomes. Transferrin is an iron transporter that is recognized by the transferrin receptor on the cell



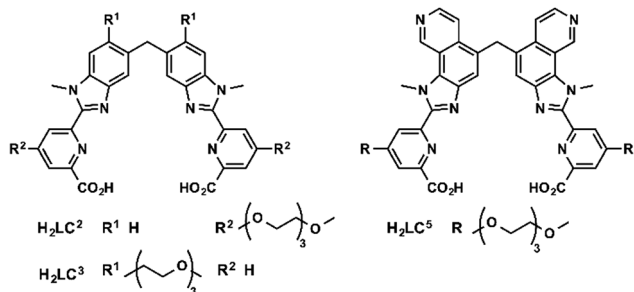


Fig. 5 Structures of  $H_2LC^n$  ligands.

membrane and internalized in CCV.<sup>26,39</sup> Thus both markers are indicative of a clathrin-mediated endocytosis. Co-localization of the helicate  $[Eu_2(LC^2)_3]$  and the probes was observed, which suggests a clathrin-mediated endocytosis. To note,  $[Ln_2(LC^2)_3]$  ( $Ln = Sm, Tb$ ) were also studied in HeLa cells and are taken up by the cell (Fig. 5).<sup>61</sup>

One limitation of  $[Eu_2(LC^2)_3]$  is its short excitation wavelength (330 nm).  $[Eu_2(LC^5)_3]$  with a pyridine moiety on the benzimidazole is excitable at lower energies (365 nm). The uptake of  $[Eu_2(LC^5)_3]$  in HeLa cells was followed by time-resolved luminescence microscopy. Similarly to  $[Eu_2(LC^2)_3]$ ,  $[Eu_2(LC^5)_3]$  was detected inside the cells after only 15 min, and showed a punctuated distribution that is consistent with an endocytic mechanism.<sup>62</sup> In another study, the uptake of  $[Eu_2(LC^3)_3]$  was investigated by measuring the brightness of the complex in cells at different temperatures (4 and 37 °C) and at different times of incubation.<sup>63</sup> As for the other helicates, a relatively rapid uptake was observed after 15 min of incubation. Shifting the temperature to 4 °C decreased the accumulation of the complex in cells, which corresponds to an active uptake mechanism. The punctuated distribution of the complex within the cell of the complex suggests an endocytic mechanism. In summary, studies of lanthanide helicates in cells demonstrate that they enter through an active mechanism, which proceeds through an endocytic pathway;  $[Eu_2(LC^2)_3]$  might enter cells *via* a clathrin-mediated endocytosis.<sup>60,61</sup>

### Azamacrocycles

Parker and co-workers investigated in depth the uptake mechanisms of  $Eu(III)$ -cyclen complexes ( $12-N_4$ ) by systematically varying the charge, lipophilicity, antenna, and bulkiness of the complexes (Fig. 6).<sup>52,53,55,64–72</sup> Most of the complexes reported enter the cell by macropinocytosis,<sup>64,67,68</sup> as demonstrated by the use of inhibitors (wortmannin, amiloride, chlorpromazine, filipin, sucrose, temperature decrease to 4–5 °C), or promoters (phorbol ester, fatty acid glycerol) of different cellular pathways and of inhibitors of endosome maturation (chloroquine, monensin). The accumulation of the complexes in cells was determined by luminescence microscopy and ICP-MS. Changes in the antenna, the linker, or the lanthanide do not seem to impact the cell uptake pathways of these complexes. However, different subcellular localization profiles have been seen, with species accumulating in lysosomes,<sup>52,55,64–68,70,72</sup> mitochondria,<sup>53,64,67,70,72</sup> or the nucleolus.<sup>64,67,68,71</sup> Some compounds

showed first an accumulation in mitochondria before relocating into lysosomes.<sup>73–75</sup> The antenna and the nature of the linker seem to play an important part in the subcellular localization of the complexes.<sup>64,67</sup> In contrast, neither the overall charge of the complex, nor the lanthanide ion influences the subcellular distribution.<sup>64,67</sup> Notably, the accumulation of complexes in the nucleoli of cells was shown to be linked with more permeable cell membranes,<sup>64</sup> which is observed in cells under stress conditions. Thus, a nucleolus localization may indicate that the complex perturbs the cell and changes the permeability of the cytoplasmic membrane.

Another prominent family of ligands is based on 9- $N_3$  complexes with pyridylalkynyl antennae.<sup>57,74–78</sup> The uptake of their lanthanide complexes occurs with macropinocytosis, in a similar manner to  $12-N_4$  complexes. These compounds are localized in mitochondria,<sup>76,77</sup> or lysosomes,<sup>74–76</sup> with some showing a redistribution from mitochondria to lysosomes over time.<sup>57,75,76</sup> Interestingly, other compounds were shown to first accumulate in mitochondria before relocating into the endoplasmic reticulum.<sup>72,76,78</sup>

In a recent paper, the impact of chirality on the cell uptake of Eu complexes was studied (Fig. 7).<sup>57</sup> The authors showed that the racemic complex  $[EuL^2]$  was taken up by the cells through macropinocytosis using various inhibitors and promoters of macropinocytosis (amiloride, wortmannin, phorbol ester, Di-Rac), clathrin-mediated endocytosis (chlorpromazine, sucrose), caveolin-dependent endocytosis (filipin), and inhibitors of the maturation of endosomes to lysosomes (chloroquine, monensin). The  $\Delta$ - and  $\Lambda$ -enantiomers of  $[EuL^2]$  and  $[EuL^1]$  were internalized to different extents and had different subcellular localization profiles. The  $\Delta$ -enantiomer of  $[EuL^2]$  showed a greater accumulation in cells as demonstrated by luminescence and ICP-MS experiments, whereas the  $\Lambda$ -enantiomer was more abundant for  $[EuL^1]$ . Macropinocytosis is not mediated by interaction with receptors at the cell surface; thus this behavior was not expected. As a potential explanation, the authors suggested that the enantiomers interact in a different manner with proteins possessing chiral binding pockets and are adsorbed to the cell surface. Thus, the internalization of one enantiomer is favored over the other. The subcellular distribution of the  $\Delta$ - and  $\Lambda$ -enantiomers of  $[EuL^2]$  and  $[EuL^1]$  was studied using confocal microscopy and organelle-specific stains. The  $\Delta$ -enantiomers accumulated preferentially in mitochondria, whereas the  $\Lambda$ -enantiomers were found in lysosomes. This difference in subcellular localization is explained by a faster relocation of the  $\Delta$ -enantiomers to the lysosomes.

Interestingly,  $[EuL^2]$  luminescence was shown to be quenched by a promoter of macropinocytosis, phorbol ester. This stresses that measuring only the brightness of Ln complexes could be misleading as no increase in luminescence is observed in cells and this could lead to the wrong conclusion regarding the uptake mechanism. This illustrates the importance of reliably quantifying the accumulation of Eu complexes in cells by a luminescence-independent method, and the need for proper controls to ensure that the increase or decrease in luminescence corresponds to an increase or decrease in uptake.



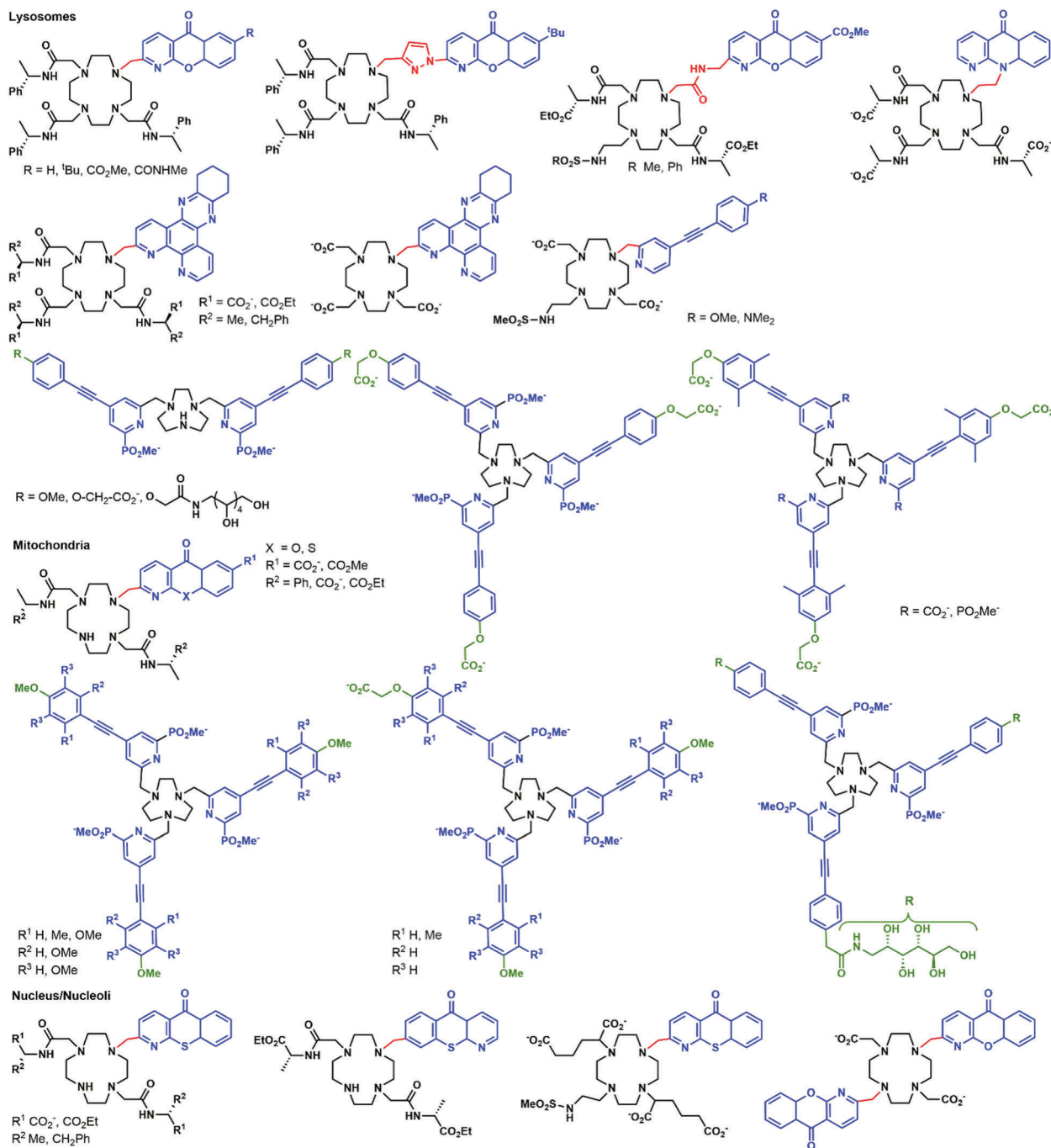


Fig. 6 Structures of complexes studied by Parker and coworkers.

$[\text{EuL}^1]$  was shown to self-aggregate in water, which quenched its luminescence. This may also occur in cells as the authors demonstrated that reduction of the concentration of incubation to  $3 \mu\text{M}$  from  $30 \mu\text{M}$  resulted in brighter images.

#### d-f heteronuclear complexes

There are numerous examples of d- and f-heteronuclear complexes with a d-block containing fragment as a light harvesting antenna and the f-element as the emitter, or that combine the luminescence of the lanthanide with the

biological activity of the d-block element.<sup>51,52</sup> Information on the uptake pathway of such complexes is scarce.<sup>53</sup>  $\text{Ln(III)-Pt(II)}$  theranostics combine Eu or Tb luminescence with the DNA-binding of the Pt moiety.<sup>53,54</sup> The uptake mechanism of the terbiplatin complex in HeLa cells was investigated using endocytic inhibitors and confocal microscopy. Chlorpromazine, cytochalasin-D, and rottlerin inhibited internalization, suggesting a macropinocytosis pathway. In HeLa and H460 cells europlatin and terbiplatin localized in the nucleoli. Based on previous work with azamacrocycles, this could be

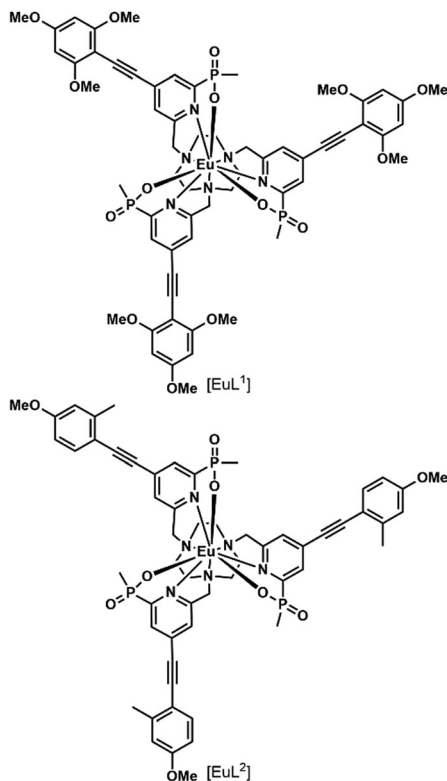


Fig. 7 Structures of  $[EuL^{1-2}]$  S- $\Delta$  enantiomers.

an indication that the complexes disturb the cells and change their permeability.<sup>34</sup>

### Prokaryotes

There are only a handful of examples of lanthanide complexes entering prokaryotic cells. We reported the internalization of a  $\beta$ -galactose-functionalized responsive Eu complex (Fig. 8).<sup>79</sup> Cleavage of the galactose by a  $\beta$ -galactosidase turned on the red Eu emission by the *in situ* formation of the sensitizing antenna. In the case of galactose-caged probes, a response was only observed in *LacZ* cells. As the enzymes were localized inside the cells, the probes had to enter the bacteria to get turned on. The probes were activated very rapidly, as when cells were incubated with 10  $\mu$ M Eu complex, the resultant Eu intensity was essentially identical at 10, 20 and 30 minutes. This suggests an uptake that is much faster than that observed for non-galactosylated complexes, which had to be incubated overnight.<sup>15</sup> However, the uptake mechanisms were not investigated for either set of complexes, and differences between the bacterial strains may contribute to some of the observed differences.

An Eu probe utilizing a similar *in situ* antenna formation strategy as the complex in Fig. 8 could be used to detect DNA and RNA. The complex was grafted onto a DNA strand, while a tris(carboxyethyl)phosphine (TCEP) was placed on a second strand. The two strands could be brought together by a complementary DNA or RNA template (the analyte), which triggered the Staudinger reduction of the azide, and the cyclization of the pre-antenna.

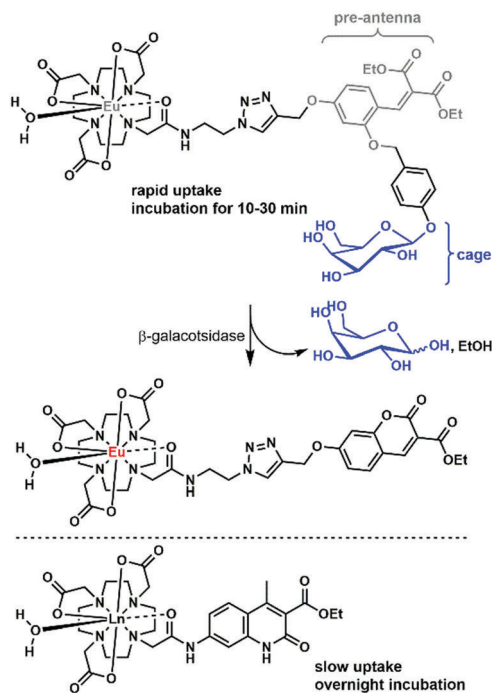


Fig. 8 Selected complexes taken up by bacteria.

The end result was the turn-on of Eu emission. This turn-on probe could be used for RNA detection in bacteria.<sup>80</sup>

### Overview

A wide variety of lanthanide complexes seems to enter cells through macropinocytosis. Helicates might enter cells through a different pathway, but this hypothesis needs further investigation. The diversity of the complexes taken up by this pathway (charges, lipophilicity, bulkiness) should point further research toward a better understanding of the parameters that drive the uptake by macropinocytosis. The cell culture medium abounds with proteins, of which albumin represents the main part. Lanthanide complexes have shown affinity for albumin.<sup>49,81</sup> Their internalization in cells could thus be driven by their interactions with proteins. The study of the speciation of the lanthanide complexes in the cell culture medium and in cells would provide valuable information that could help decipher the pathways by which they internalized. In this regard, the tools developed to study the mode of action of metallodrugs, *e.g.* mass spectrometry-based techniques, can be used to study Ln complexes.<sup>82</sup>

## Methods of lanthanide delivery

### Complexes targeted to the exterior of the cell

There are numerous reports detailing the inability of 'free' lanthanide(III) ions to enter intact cells. Similarities between spectroscopically silent  $Ca^{2+}$  and versatile lanthanides have enabled the investigation of calcium-binding sites in cell membranes and calcium channels.<sup>83,84</sup> Significant differences are often seen within the lanthanide series due to the decrease in



the ionic radius from 106 ppm to 86 ppm upon going from  $\text{La}^{3+}$  to  $\text{Yb}^{3+}$ .<sup>84,85</sup> In the absence of the ionophore A23187, at concentrations up to 400  $\mu\text{M}$ ,  $\text{Yb}^{3+}$ ,  $\text{Tb}^{3+}$ ,  $\text{Eu}^{3+}$ ,  $\text{La}^{3+}$ ,  $\text{Sm}^{3+}$  and  $\text{Gd}^{3+}$  were unable to mimic  $\text{Ca}^{2+}$  in triggering  $\text{K}^{+}$ -release. In the presence of A23187 even concentrations  $<10 \mu\text{M}$  were sufficient, in accord with the ionophore being necessary for the lanthanides to enter the cell.<sup>86</sup> In a study on the effect of lanthanide(III) ions on insulin release in  $\beta$ -cells the localization of  $\text{Sm}^{3+}$  and  $\text{Tm}^{3+}$  was confirmed to be restricted to the plasma membrane by electron microscopy.<sup>85</sup>  $\text{EuCl}_3$  (pH 7.4 solution) and the complex of Eu with albumin had different distributions when injected intravenously into rats. The salt was taken up by the liver, while the albumin complex was excreted rapidly into the urine, suggestive of a weak interaction between  $\text{Eu}^{3+}$  and albumin in serum.<sup>87</sup> Intriguingly,  $\text{La}_2(\text{CO}_3)_2$  is a potential non-calcium phosphate binding drug. Its surprisingly low systemic toxicity is ascribed to its low solubility in physiological fluids. The resulting  $[\text{La}^{3+}] < 3 \text{ pm L}^{-1}$  is low enough to make the lanthanide's calcium-like behaviour negligible.<sup>88</sup>

Despite free lanthanides in general being cell-impermeable, Cheng *et al.* found by confocal scanning microscopy that erythrocytes are in fact permeable to these ions.<sup>89</sup> Intracellular fluorescein fluorescence (introduced by labelling with fluorescein isothiocyanate) was quenched by uncomplexed lanthanides in a size- and total orbital angular momentum-dependent fashion. Overall anionic species, such as the  $-3$  charged dicitrate complexes, were even more effective, as they could enter cells *via* anion channels.<sup>89</sup>

In prokaryotes systematic studies are lacking. However, electrogenic  $\text{Ca}^{2+}$  uptake in *Azotobacter vinelandii* was inhibited by  $\text{LaCl}_3$ ,  $\text{TbCl}_3$  and  $\text{PrCl}_3$  (20  $\mu\text{M}$ ) due to the similarity of the lanthanide(III) ions to the natural substrate. However, the presence of Ln, Tb or Pr was not investigated in the cells.<sup>90</sup>

Parker and collaborators from Cisbio Bioassays synthesized *para*-substituted aryl-alkynyltriazacyclononane (TACN) Eu(III) complexes.<sup>91</sup> These highly water-soluble carboxylated or sulfonated complexes had overall negative charges, which prevent nonspecific binding to the cell membrane. Binding to the cholecystokinin 2 receptor (CCK2) expressed in the membrane of the HEK293 cells was possible with SNAP-tag technology. Successful binding was confirmed by time resolved FRET microscopy with the Eu(III) as the donor and a red fluorescent agonist of CCK2 as the acceptor.<sup>91</sup>

In another study, eight Gd-DOTA derivatives were prepared that targeted the metabotropic glutamate receptor subtype 5 (mGluR5).<sup>92</sup> mGluR5 is part of the excitatory glutamate neurotransmitter system, involving emotions, the cognitive and motivation actions of the brain. Gd-DOTA complexes with a glutarate arm (Gd-DOTA-GA) were linked to specific allosteric antagonists of mGluR5. The complexes were tested in rat astrocytes. Two of the eight complexes bound selectively to the receptor and were taken up by the cells.<sup>92</sup>

Covalent membrane labelling of HEK293 cells was also possible with upconverting nanocrystals (UCNs) doped with  $\text{Nd}^{3+}$ .<sup>93</sup> The crystals can absorb 808 nm light and emit at 480 nm, have a minimized absorption of water, and are inert

to thermal effects, unlike other UCNs that absorb 980 nm light. Membrane labelling was achieved by azide-alkyne cycloaddition. Cell-surface azides were introduced metabolically from *N*-azidoacetylmanosamine, and reacted with dibenzylcyclo-octyne-functionalized UCNs. The membrane localization was confirmed by confocal microscopy and flow cytometry (FMS) analysis. UCNs bound to the membrane could act as NIR-activatable photoswitches. The emission wavelength of the UCNs matches the absorption of channelrhodopsin-2 (ChR2, 480 nm), which enabled remote control in zebrafish larvae of calcium channels expressing light-gated ChR2.<sup>93</sup> Interestingly, PEG-phospholipid-coated UCNs not covalently anchored to the membrane are taken up most likely by nonspecific endocytosis.<sup>94</sup>

MRI contrast agents that label the cell membrane are interesting alternatives to tags targeting intracellular structures. Gd complexes attached to hydrophobic 4-, 10-, or 12-carbon alkyl chains were prepared.<sup>95</sup> Low micromolar concentrations of these complexes with 10- or 12-carbon chains labelled the cell membranes of a range of adhering and non-adhering cells within 40 min. DFRET confirmed that the complexes bound to the membrane with the metal site facing the extracellular place, while the hydrophobic parts were arranged in the membrane. The labelled cells had normal doubling times and their morphologies were normal compared to the control cells.<sup>95</sup>

### Small molecule targeting

Numerous receptors are known to be overexpressed in malignant cells. Lanthanide probes bearing specific targeting moieties can help with the detection of these cells. One such overexpressed receptor is the folate receptor (FR), which has a high affinity for folic acid (FA). When lanthanide complexes were attached to a folic acid targeting moiety, compounds with shorter FA-chelate distances were more efficiently internalized.<sup>96</sup> It was also found that synthetically more accessible pteric acid (PTE) functionalized complexes are suboptimal substitutes for folic acid, since lower cellular uptake could be observed for these species.<sup>96</sup> When Eu chelates were bound to three different positions of FA, no noticeable difference between the cellular uptakes of the compounds could be seen.<sup>97</sup> The substitution of FA with methotrexate (MTX), an anti-folate, resulted in higher cytotoxicity for all the MTX complexes compared to their corresponding FA ones.<sup>98</sup>

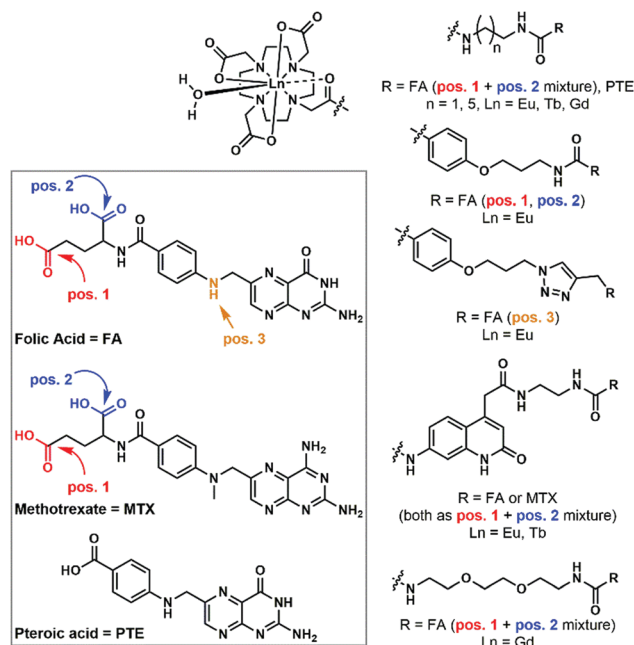
In all cases, where incubation was performed on both FR(−) and FR(+) cells,<sup>97,98</sup> selective internalization in FR(+) cells could be observed. This, and a reduced amount of cellular uptake when competing experiments with free FA were performed, indicates that the FA complexes are internalized through a FR-mediated mechanism.<sup>99</sup> In the latter, the molecules are taken up by caveolae, and after binding with the FR and sealing the compartment, the ligand gets dissociated from the FR using a proton pump. This induces ligand transport *via* the reduced folate carrier (RFC), an anion exchange channel. This mechanism is somewhat controversial, since in certain cell lines, coupling of FR and RFC has been observed;<sup>100,101</sup> in others it has been concluded that they work independently.<sup>102,103</sup> High cellular



Progesterone receptors (PR) can be found inside the cells. Steroid conjugated contrast agents are used for magnetic resonance imaging. The conjugation with these target moieties increases the ability of Gd chelates to associate with cells.<sup>111,112</sup> Although the cellular uptake mechanism is still unclear, all experiments<sup>111,113–115</sup> show moderately selective uptake for PR(+) cells, indicating that the presence of those receptors has an influence on the internalization. More hydrophilic complexes had lower cytotoxicity, but also lower membrane permeability.<sup>111,113–115</sup> An overall negative charge on the complex decreased the internalization (Fig. 9).<sup>115</sup>

Cell penetrating peptides (CPPs) are <30 residue peptides that can cross the cell membrane or carry cell-impermeable cargos through the cell membrane.<sup>116</sup> The majority have high positive charges and interact electrostatically with membrane proteins. A range of CPPs are known: some are derived from proteins, some are the combination of different protein parts, and some are synthetic (Table 1).<sup>41,117</sup> So far no chimeric peptides have been used for metal uptake.

Studies of the uptake mechanisms of CPPs have shown that they are taken up by cells *via* different pathways as evidenced by the parameters that influence the uptake mechanism.<sup>116,118,119</sup> In particular, the uptake mechanism does not depend on the type of peptide used, but rather on the combination of the cargo and the peptide, interactions with the cell membrane components (lipids, proteins, polysaccharides), and the local concentration of the peptide.<sup>116,118,119</sup> At low concentrations (below 2  $\mu\text{M}$ ) direct translocation seems to be favoured,<sup>118</sup>



whereas at higher concentrations (10  $\mu\text{M}$  and above) CPPs are taken up by endocytosis. This criterion is not exclusive however, and both uptake mechanisms can be observed at the same time.<sup>116,118,119</sup> At higher concentrations, the transduction mechanism, the direct uptake of CPPs dependent of intracellular processes, has also been described.<sup>118</sup>

Peptides can help metal complexes cross the membrane and can precisely target one subcellular localisation (Table 1). The nucleus can be targeted with Nuclear Localisation Sequences (NLSs) such as SV40<sup>73,120,121</sup> appended to the CPPs. When this sequence is used in combination with lanthanides, a second sequence performs the role of membrane transport. The HIV Trans Activator of the Transcription (Tat) peptide shows also a predominant localisation in the nucleus. The synthetic mitochondria targeted peptide (Mitochondria Penetrating Peptide (MPP))<sup>122</sup> sequence is composed of an alternating sequence of a synthetic cyclohexylalanine residue and a D-arginine or a lysine. The lipophilicity of MPP facilitates subcellular targeting, as a high  $\log P$  is beneficial for mitochondrial localization, whereas low  $\log P$  peptides stay in the cytoplasm and in the nuclei. The threshold value depends on the complex charge. These peptides had carried a Ru complex cargo.<sup>123</sup> The guanidinium protein linked to a complex co-localizes with MitoTracker Orange in mitochondria.<sup>124</sup> Poly-lysine with human transferrin and poly-lysine with Gd-DTPA were added onto a luciferase plasmid.<sup>125</sup> The concentration of the Gd complex on poly-lysine had to be chosen carefully so as not to interfere with the interaction between the DNA polyanion and the cationic lysine polymers. The plasmid was taken up by the cells *via* the transferrin receptors. The co-transport of DNA and the MRI contrast agent was efficient, as with each plasmid more than a thousand metal complexes are taken up.

**Table 1** Cell penetrating peptide sequences for transporting metal complexes into cells

Name	Sequence	Target organelle	Metal cargo	Ref.
Peptides derived from proteins				
<i>TPU</i>	RQVKIWFQNRRMKQKK	Nucleus	Lanthanide	121
<i>Tat</i> <sub>49–57</sub>	RKKRRQRRR		Ln, Zn, Tc, Rh	132–135
<i>pVEC</i>	LLIILRRRIRKQAHASHK		—	—
NLS				
<i>ALL1</i>	RKRKRK		Lanthanide	120
<i>SV40T</i>	KKKRKVK		Co, Tc	136–138
Chimeric peptides				
<i>Transportan</i>	GWTLNSAGYLLGKINLKALAALAKKIL	—	—	—
<i>Pep-1</i>	KETWWETWWTEWSQPKKKRKV	—	—	—
<i>MPG</i>	GALFLGFLGAAGSTMGAWSQPKKKRKV	—	—	—
Synthetic peptides				
PolyArg	RRR· · ·RRR	—	Lanthanide, Ru	51, 73, 112, 127 and 139–141
MAP	KLALKLALKALKAAKLKA		—	—
R6W3			—	—
MPP	F <sub>x</sub> rF <sub>x</sub> KF <sub>x</sub> rF <sub>x</sub> K	Mitochondria	Ru	123
Guanidinium		Perinuclear	Lanthanide	51, 124

Mohandessi *et al.* reported the concentration-dependent passive cytoplasmic delivery of a Tb(III) complex functionalized with cell-penetrating peptides in MDCKII cells.<sup>126</sup> At high incubation concentrations (20–60  $\mu$ M instead of 5  $\mu$ M), a diffuse distribution throughout the cytoplasm was observed by time-resolved fluorescence microscopy. Decreasing the temperature to 4 °C did not influence the concentration of the complex in cells, suggesting that a passive energy-independent mechanism takes place, which could be attributed to a transduction mechanism.<sup>118</sup>

Complex diffusion inside the cells is improved upon liberation of the cargo from the peptide. For this, disulfide bonds between the complex and the peptide sequence can be cleaved by intracellular thiols.<sup>120,127</sup> Molecules with disulfide bonds stay longer in cells than those without, which could be interesting for imaging.

Peptides can be cytotoxic. This can be an advantage if targeting cancer cells; however, it can be a problem for imaging. Natural CPPs have a low toxicity, while the Tat sequence is known to induce apoptosis of hippocampal neurons<sup>128,129</sup> and poly-Arg can induce microvascular macromolecule leakage.<sup>130</sup> With this in mind, a lanthanide complex was equipped with two NLSs: ALL1 to improve the cellular uptake and SV40 to target the nucleus.<sup>120</sup> To avoid an immune response, a human homologue (87% similar) to the Penetratin, a CPP from the Antennapedia homeodomain, was used to transport a contrast agent.<sup>121</sup>

The peptide can also be toxic for organelles. Mitochondria are sensitive to the hydrophobicity of MPP: highly hydrophobic compounds induce membrane disruption and apoptosis, whereas high concentrations of less hydrophobic ones can modify the membrane potential.<sup>131</sup> These factors need to be taken into account when choosing the CPP.

### Intracellular imaging with macromolecules

Biological material has low autofluorescence in the NIR region, which means that signals from lanthanides can be easily

differentiated from signals from the cells; there is a good signal-to-noise ratio and good detection sensitivity. Another advantage is that NIR photons have minimal interaction with biological media so will not perturb the live cells, and they scatter less than photons from the visible range. The NIR emitting lanthanides have low intrinsic quantum yields and are extremely sensitive to quenching with X–H oscillators (X = O, N, C). One way to overcome the often low brightness of these NIR emitters is to incorporate a large number of absorbing and emitting units into supramolecular edifices. Three types of supramolecular materials will be discussed: metal–organic frameworks, metallacrowns and dendrimers.

**MOFs.** Metal–organic frameworks (MOFs) are ordered, highly porous solids consisting of organic linkers and metal counterparts with large pore volumes and surface areas, and the possibility for surface functionalization.<sup>142</sup> By integrating the luminescent features of lanthanide ions with chromophoric linkers, highly luminescent compounds can be made where the lanthanides are sensitized by the antenna effect – this way a large number of cations can be clustered in a small volume, which yields a large number of photons emitted per unit volume.<sup>143</sup>

One of the key requirements of a MOF is that it should enter the cells and release its cargo efficiently. Nanoparticles enter cells *via* endocytosis.<sup>144</sup> Endocytosis can occur on a macro- or microscale; as far as MOFs are concerned the process is on a microscale. Microscale endocytosis can be divided into groups depending on the protein coating on the vesicles that form upon cell penetration.<sup>144</sup>

The effect of functionalizing and extending the organic 1,4-benzenedicarboxylate (BDC) linker of a Zr-based MOF, UiO-66, on cellular uptake was investigated.<sup>145</sup> The fluorescent and hydrophilic molecule calcein was used in conjunction with flow cytometry analysis and confocal microscopy to determine the efficiency of MOF internalization. The Zr-MOFs were functionalized with –NO<sub>2</sub>, –Br and –NH<sub>2</sub>, or their linkers were



extended with naphthalene-2,6-dicarboxylic acid or 4,4'-biphenyl-dicarboxylic acid and incubated with HeLa cells. MOFs with functionalized ligands were internalized more efficiently than MOFs with extended linkers. However, they were more susceptible to lysosomal degradation, to which extended linker MOFs were resistant. Increasing uptake efficiency with decreasing particle size was found. Increased granularity was seen by flow cytometry for larger MOFs compared to smaller ones.<sup>145</sup> These results on surface chemistry modifications should be applicable to lanthanide-based MOFs.

The first sensitized NIR emission came from Yb<sup>3+</sup>-containing MOFs. The MOF structure could be varied while keeping the chromophore linker the same, which tuned the photophysical properties of the MOFs by modifying the structures.<sup>146</sup> The ligand used was 4,4'-[(2,5-dimethoxy-1,4-phenylene)di-2,1-ethenediyl]bis-benzoic acid (H<sub>2</sub>PVDC), due to its ability to absorb strongly in the visible range and to sensitize the Yb<sup>3+</sup>. X-ray diffraction showed that Yb-PVDC-1 crystallized in the high symmetry Fddd space group, and the chains are made up of alternating octa- and hexa-coordinated Yb<sup>3+</sup> ions, with the octa-coordinated ions having two water molecules coordinated. The arrangements of the ligands could allow for weak interactions between one another, possibly decreasing the excitation energy. A second MOF, Yb-PVDC-2, was also synthesized, which still contained octa- and hexa-coordinated Yb<sup>3+</sup> ions, but the ligands were then parallel. The lowest energy excitation of Yb-PVDC-2 red-shifted to 500 nm, compared to 470 nm in Yb-PVDC-1, possibly due to the close  $\pi$ - $\pi$  interactions. The quantum yield of Yb-PVDC-2 was five times higher than that of Yb-PVDC-1, which is most likely due to the coordinated water molecules, which are absent in Yb-PVDC-2.<sup>146</sup>

Yb-PVDC-3 was prepared *via* reverse microemulsion synthesis, which yielded a nanoscale version of the MOF that could be used for imaging in living cells.<sup>143</sup> Lifetime measurements show that the Yb<sup>3+</sup> are in two types of environments. Those with longer lifetimes are in the inside of the MOF structure, and those with shorter lifetimes are on the edges/faces of the MOF. The external Yb<sup>3+</sup> ions are more susceptible to quenching from their surroundings; this explains their shorter lifetime values.

Nano-Yb-PVDC-3 exhibited both biological stability and photostability, and had an IC<sub>50</sub> of 100  $\mu\text{g L}^{-1}$ , which is suitable for live cell imaging. Nano-Yb-PVDC-3 was incubated with HeLa and NIH3T3 cells. Confocal microscopy and inductively coupled plasma measurements show that nano-Yb-PVDC-3 is indeed internalized into the cell. Further analysis is required to examine the mechanism of cell penetration. The quantum yields for the nanoMOF are reported to be relatively low:  $1.0 (\pm 0.3) \times 10^{-4}$  in water and  $5.2 (\pm 0.8) \times 10^{-5}$  in aqueous 0.1 M Hepes buffer. This is where the advantage of using a MOF comes into play, as it maximizes the number of cations and chromophores per unit volume, which increases the number of emitted photons to the level that Yb luminescence is readily detected even in such challenging milieux.

Yb-PVDC-3 was photostable. Stability in cells was tested by monitoring the cells with SEM. As the lanthanide emission can only be detected if it is sensitized by the antenna, the fact that emission could be detected throughout the test meant that the

MOF remained intact in the cell and is therefore biologically stable.

**Metallacrowns.** Metallacrowns are structural analogues to crown ethers, built up of a repeating unit  $[\text{M}-\text{N}-\text{O}]_n$ , where the metal (M) and nitrogen (N) replace the carbon atoms of the crown ether.<sup>147</sup> The incorporation of lanthanide central metals imparts luminescent properties to the supramolecule, while the organic building blocks provide a handle for controlling the absorption properties.<sup>148,149</sup> The extended structure provides excellent shielding from quenching oscillators, even including C-H ones.<sup>150</sup>

So far the use of metallacrowns in cells has been limited to necrotic cells, where they are used as alternative cell markers. Detection of cell necrosis is important so as to determine cell viability. Currently used is propidium iodide,<sup>151</sup> an organic fluorophore that is susceptible to rapid photobleaching, to which lanthanide-based metallacrowns are resistant.

Recently, a series of lanthanide metallacrowns with the  $\text{Ln}^{3+}[\text{Zn}(\text{II})\text{MCquinHA}]$  structure (where  $\text{Ln}^{3+} = \text{Nd}, \text{Er}, \text{Yb}$ ) were synthesized. The quin ligand enables excitation with low energy light, while the rigid structure that keeps solvent molecules away from the lanthanide afforded high quantum yields.<sup>150</sup> While these complexes were poorly water soluble, a new generation of metallacrowns could overcome this problem.<sup>152</sup> By replacing the chromophoric linker with the one based on pyrazinehydroxamic acid (H<sub>2</sub>pyzHA), highly water-soluble compounds ( $\text{Ln}^{3+}[\text{Zn}(\text{II})\text{MCpyzHA}]$ ,  $\text{Ln}^{3+} = \text{Yb}, \text{Nd}$ ) were obtained that maintained the impressive NIR luminescence of their predecessors. HeLa cells were incubated with  $\text{Yb}^{3+}[\text{Zn}(\text{II})\text{MCpyzHA}]$  to examine necrotic cell accumulation, cell viability and photostability. It was found the metallacrowns were both photophysically and biologically stable.<sup>152</sup> This metallacrown was also found, in a separate study, to be suitable for *in vivo* cell fixation and counterstaining upon exposure to UVA light.<sup>153</sup>

**Dendrimers.** Dendrimers are highly branched polymeric materials used for catalysis and drug delivery and as biosensors and vectors.<sup>154,155</sup> They are good candidates for use in living cells as one can attach functional groups for increased solubility, cellular uptake control and organelle localization.<sup>16</sup> Dendrimers with cationic charge tend to be toxic to cells, whereas anionic dendrimers, which usually have carboxylate dendrons, are not cytotoxic.<sup>154</sup>

Examples for the incorporation of NIR-emitting lanthanide ions into dendrimers are scarce. Two dendrimers based on cyclam cores with PAMAM appendages and incorporating  $\text{Nd}^{3+}$  were designed. Dansyl4 and a larger Dansyl8 were synthesised; the former was able to coordinate  $\text{Nd}^{3+}$  but unable to sensitize it, whereas by increasing the number of chromophoric dendrons from four to eight, sensitisation was seen.<sup>156</sup> No investigations into the biological applications of these molecules have been reported, most likely due to the unfavourable cationic nature of the compounds.

Substituting parts of PAMAM with a total of 32 2,3-naphthalimide chromophores gave rise to a dendrimer which was capable of accommodating eight lanthanide ions.<sup>157</sup> Photophysical studies



showed that the triplet states of the ligands were at a particularly favourable energy position for Sm<sup>3+</sup> sensitization. Sm(III)-G3P-2,3-Nap exhibited sharp visible and NIR emission bands. The emission was shown to be sensitized by the chromophores of the dendrimer. Furthermore, an Alamar Blue assay of HeLa and NIH3T3 cells showed that cell viability was higher than 95% at a concentration of 1 μM and the dendrimer was non-toxic up to 24 h, indicating that the compound can be used for live cell imaging. Confocal microscopy showed that the probe was taken up by cells and most likely distributed amongst lysosomes.

## Conclusions

The transition from a test tube to living cells is a challenging one even for a selective, sensitive, highly water-soluble chemical probe. The requirements placed on lanthanide complexes by the delicate homeostasis of the cells are stringent. Not only do they have to perform to a comparable extent in the biological medium as they do in buffered water, but they have to be non-toxic, they have to be resistant to degradation for the period of the experiment, and they should not produce degradation products that interfere with the system under investigation.

A special challenge is due to the fact that many of the currently available lanthanide probes are coordination complexes with the possibility of dissociating in dilute solutions. Therefore, thermodynamic data on complexes with new ligand systems are highly valuable. Of note, several recent reports have detailed the uptake of moderately stable complexes of simple bi- and tridentate ligands into living cells.<sup>158,159</sup> Given the synthetic accessibility of these systems, and the efficiency with which they are internalized, it would be of great importance to understand the role of these attractively simple ligands in cellular uptake, and to investigate whether their benefits could be transferred to traditional tri- and tetraazamacrocyclic ligands.

There are still large unexplored areas in this field, from the factors governing complex uptake and egress in bacteria to the fates of the probes in both eukaryotic and prokaryotic cells. Recently emerging lanthanide(III) based smart contrast agents open up new avenues of investigation due to their larger, softer metal ions and the classes of ligands that accommodate them.<sup>9,160</sup> These structural features, as well as their accessible redox chemistry, will likely impact their biological behaviour.

## Conflicts of interest

There are no conflicts to declare.

## Acknowledgements

This work was supported by the Swedish Research Council (project grant 2017-04077 to K. E. B.) and the Carl Tryggers Foundation (postdoctoral fellowship for E. M.). E. D., D. P. and D. S. are Erasmus students. The Ecole Normale Supérieure

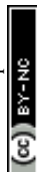
(Paris, <http://www.chimie.ens.fr/?q=en>) is gratefully acknowledged for financial support through an Erasmus fellowship to A. S. We thank Daniel Kovacs for collecting the spectra in Fig. 1.

## Notes and references

- 1 L. Burai, R. Scopelliti and E. Toth, *Chem. Commun.*, 2002, 2366–2367.
- 2 E. Toth, L. Burai and A. E. Merbach, *Coord. Chem. Rev.*, 2001, **216**–217, 363–382.
- 3 L. Burai, E. Toth, S. Seibig, R. Scopelliti and A. E. Merbach, *Chem. – Eur. J.*, 2000, **6**, 3761–3770.
- 4 S. Seibig, E. Toth and A. E. Merbach, *J. Am. Chem. Soc.*, 2000, **122**, 5822–5830.
- 5 ed. A. Merbach, L. Helm and E. Toth, *The Chemistry of Contrast Agents in Medical Magnetic Resonance Imaging*, John Wiley & Sons Ltd, 2013.
- 6 L. A. Ekanger, L. A. Polin, Y. Shen, E. M. Haacke, P. D. Martin and M. J. Allen, *Angew. Chem., Int. Ed.*, 2015, **54**, 14398–14401.
- 7 L. A. Ekanger, L. A. Basal and M. J. Allen, *Chem. – Eur. J.*, 2017, **5**, 1145–1150.
- 8 L. A. Ekanger, D. R. Mills, M. M. Ali, L. A. Polin, Y. Shen, E. M. Haacke and M. J. Allen, *Inorg. Chem.*, 2016, **55**, 9981–9988.
- 9 M. J. Allen, *Synlett*, 2016, 1310–1317.
- 10 A. N. W. Kuda-Wedagedara, C. Wang, P. D. Martin and M. J. Allen, *J. Am. Chem. Soc.*, 2015, **137**, 4960–4963.
- 11 A. de Bettencourt-Dias, *Luminescence of Lanthanide Ions in Coordination Compounds and Nanomaterials*, John Wiley & Sons Ltd, 2014, ch. 01, pp. 1–48.
- 12 K. Binnemans, *Coord. Chem. Rev.*, 2015, **295**, 1–45.
- 13 A. Beeby, S. W. Botchway, I. M. Clarkson, S. Faulkner, A. W. Parker, D. Parker and J. A. G. Williams, *J. Photochem. Photobiol., B*, 2000, **57**, 83–89.
- 14 D. Kovacs and K. E. Borbas, *Coord. Chem. Rev.*, 2018, **364**, 1–9.
- 15 D. Kovacs, X. Lu, L. S. Mészáros, M. Ott, J. Andres and K. E. Borbas, *J. Am. Chem. Soc.*, 2017, **139**, 5756–5767.
- 16 R. M. Supkowski and W. D. Horrocks, Jr., *Inorg. Chim. Acta*, 2002, **340**, 44–48.
- 17 A. Beeby, I. M. Clarkson, R. S. Dickins, S. Faulkner, D. Parker, L. Royle, S. A. S. de, J. A. G. Williams and M. Woods, *J. Chem. Soc., Perkin Trans. 2*, 1999, 493–504.
- 18 J.-C. G. Bunzli, *Coord. Chem. Rev.*, 2015, **293**–294, 19–47.
- 19 J.-C. G. Bunzli and S. V. Eliseeva, in *Lanthanide Luminescence: Photophysical, Analytical and Biological Aspects*, ed. P. Hänninen and H. Härmä, Springer, Berlin, Heidelberg, 2011, pp. 1–45.
- 20 K. Y. Zhang, Q. Yu, H. Wei, S. Liu, Q. Zhao and W. Huang, *Chem. Rev.*, 2018, **118**, 1770–1839.
- 21 E. Pershagen and K. E. Borbas, *Coord. Chem. Rev.*, 2014, **273**–274, 30–46.
- 22 M. Sy, A. Nonat, N. Hildebrandt and L. J. Charbonniere, *Chem. Commun.*, 2016, **52**, 5080–5095.
- 23 M. Rajendran, E. Yapici and L. W. Miller, *Inorg. Chem.*, 2014, **53**, 1839–1853.
- 24 S. Shuvaev, M. Starck and D. Parker, *Chem. – Eur. J.*, 2017, **23**, 9974–9989.
- 25 N. Sim and D. Parker, *Chem. Soc. Rev.*, 2015, **44**, 2122–2134.
- 26 C. A. Puckett, R. J. Ernst and J. K. Barton, *Dalton Trans.*, 2010, **39**, 1159–1170.
- 27 K. Hanaoka, K. Kikuchi, S. Kobayashi and T. Nagano, *J. Am. Chem. Soc.*, 2007, **129**, 13502–13509.
- 28 M. Rajendran and L. W. Miller, *Biophys. J.*, 2015, **109**, 240–248.
- 29 G. Nivriti and L. W. Miller, *Cytometry, Part A*, 2010, **77**, 1113–1125.
- 30 G.-L. Law, K.-L. Wong, C. W.-Y. Man, W.-T. Wong, S.-W. Tsao, M. H.-W. Lam and P. K.-S. Lam, *J. Am. Chem. Soc.*, 2008, **130**, 3714–3715.
- 31 L.-O. Palsson, R. Pal, B. S. Murray, D. Parker and A. Beeby, *Dalton Trans.*, 2007, 5726–5734.
- 32 A. D'Aléo, A. Picot, A. Beeby, J. A. Gareth Williams, B. Le Guennic, C. Andraud and O. Maury, *Inorg. Chem.*, 2008, **47**, 10258–10268.
- 33 A. D'Aléo, A. Bourdolle, S. Brustlein, T. Fauquier, A. Grichine, A. Duperray, P. L. Baldeck, C. Andraud, S. Brasselet and O. Maury, *Angew. Chem., Int. Ed.*, 2012, **51**, 6622–6625.



- 34 A. Grichine, A. Haeefe, S. Pascal, A. Duperray, R. Michel, C. Andraud and O. Maury, *Chem. Sci.*, 2014, **5**, 3475–3485.
- 35 A. Jana, E. Baggaley, A. Amoroso and M. D. Ward, *Chem. Commun.*, 2015, **51**, 8833–8836.
- 36 A. T. Bui, A. Grichine, A. Duperray, P. Lidon, F. Riobe, C. Andraud and O. Maury, *J. Am. Chem. Soc.*, 2017, **139**, 7693–7696.
- 37 E. R. H. Walter, J. A. G. Williams and D. Parker, *Chem. Commun.*, 2017, **53**, 13344–13347.
- 38 Y. Ning, J. Tang, Y.-W. Liu, J. Jing, Y. Sun and J.-L. Zhang, *Chem. Sci.*, 2018, **9**, 3742–3753.
- 39 I. A. Khalil, K. Kogure, H. Akita and H. Harashima, *Pharmacol. Rev.*, 2006, **58**, 32–45.
- 40 T.-G. Iversen, T. Skotland and K. Sandvig, *Nano Today*, 2011, **6**, 176–185.
- 41 C. Bechara and S. Sagan, *FEBS Lett.*, 2013, **587**, 1693–1702.
- 42 V. P. Torchilin, R. Rammohan, V. Weissig and T. S. Levchenko, *Proc. Natl. Acad. Sci. U. S. A.*, 2001, **98**, 8786–8791.
- 43 D. L. Foxall, K. M. Brindle, I. D. Campbell and R. J. Simpson, *Biochim. Biophys. Acta*, 1984, **804**, 209–215.
- 44 A. Mohamadi and L. W. Miller, *Bioconjugate Chem.*, 2016, **27**, 2540–2548.
- 45 H. E. Rajapakse, N. Gahlaut, S. Mohandessi, D. Yu, J. R. Turner and L. W. Miller, *Proc. Natl. Acad. Sci. U. S. A.*, 2010, **107**, 13582–13587.
- 46 V. Placide, A. T. Bui, A. Grichine, A. Duperray, D. Pitrat, C. Andraud and O. Maury, *Dalton Trans.*, 2015, **44**, 4918–4924.
- 47 T. Zhang, X. Zhu, C. C. W. Cheng, W.-M. Kwok, H.-L. Tam, J. Hao, D. W. J. Kwong, W.-K. Wong and K.-L. Wong, *J. Am. Chem. Soc.*, 2011, **133**, 20120–20122.
- 48 B. Song, G. Wang, M. Tan and J. Yuan, *J. Am. Chem. Soc.*, 2006, **128**, 13442–13450.
- 49 R. A. Poole, C. P. Montgomery, E. J. New, A. Congreve, D. Parker and M. Botta, *Org. Biomol. Chem.*, 2007, **5**, 2055–2062.
- 50 R. A. Poole, G. Bobba, M. J. Cann, J.-C. Frias, D. Parker and R. D. Peacock, *Org. Biomol. Chem.*, 2005, **3**, 1013–1024.
- 51 F. Kiehl, A. Congreve, G.-L. Law, E. J. New, D. Parker, K.-L. Wong, P. Castreño and J. D. Mendoza, *Chem. Commun.*, 2008, 2435–2437.
- 52 F. Kiehl, G.-L. Law, E. J. New and D. Parker, *Org. Biomol. Chem.*, 2008, **6**, 2256–2258.
- 53 D. G. Smith, G.-L. Law, B. S. Murray, R. Pal, D. Parker and K.-L. Wong, *Chem. Commun.*, 2011, **47**, 7347–7349.
- 54 G.-L. Law, D. Parker, S. L. Richardson and K.-L. Wong, *Dalton Trans.*, 2009, 8481–8484.
- 55 E. J. New, D. Parker and R. D. Peacock, *Dalton Trans.*, 2009, 672–679.
- 56 J. Yu, D. Parker, R. Pal, R. A. Poole and M. J. Cann, *J. Am. Chem. Soc.*, 2006, **128**, 2294–2299.
- 57 A. T. Frawley, H. V. Linford, M. Starck, R. Pal and D. Parker, *Chem. Sci.*, 2018, **9**, 1042–1049.
- 58 M. Groessl and C. G. Hartinger, *Anal. Bioanal. Chem.*, 2013, **405**, 1791–1808.
- 59 J.-C. G. Bünzli, *Interface Focus*, 2013, **3**, 20130032.
- 60 B. Song, C. D. B. Vandevyver, A.-S. Chauvin and J.-C. G. Bünzli, *Org. Biomol. Chem.*, 2008, **6**, 4125–4133.
- 61 A.-S. Chauvin, S. Comby, B. Song, C. D. B. Vandevyver and J.-C. G. Bünzli, *Chem. – Eur. J.*, 2008, **14**, 1726–1739.
- 62 E. Deiters, B. Song, A.-S. Chauvin, C. D. B. Vandevyver, F. Gummy and J.-C. G. Bünzli, *Chem. – Eur. J.*, 2009, **15**, 885–900.
- 63 A.-S. Chauvin, S. Comby, B. Song, C. D. B. Vandevyver, F. Thomas and J.-C. G. Bünzli, *Chem. – Eur. J.*, 2007, **13**, 9515–9526.
- 64 E. J. New, D. Parker, D. G. Smith and J. W. Walton, *Curr. Opin. Chem. Biol.*, 2010, **14**, 238–246.
- 65 S. Shuvaev, R. Pal and D. Parker, *Chem. Commun.*, 2017, **53**, 6724–6727.
- 66 D. G. Smith, B. K. McMahon, R. Pal and D. Parker, *Chem. Commun.*, 2012, **48**, 8520–8522.
- 67 E. J. New, A. Congreve and D. Parker, *Chem. Sci.*, 2010, **1**, 111–118.
- 68 E. J. New and D. Parker, *Org. Biomol. Chem.*, 2009, **7**, 851–855.
- 69 C. P. Montgomery, E. J. New, L. O. Palsson, D. Parker, A. S. Batsanov and L. Lamarque, *Helv. Chim. Acta*, 2009, **92**, 2186–2213.
- 70 C. P. Montgomery, B. S. Murray, E. J. New, R. Pal and D. Parker, *Acc. Chem. Res.*, 2009, **42**, 925–937.
- 71 R. Pal and D. Parker, *Org. Biomol. Chem.*, 2008, **6**, 1020–1033.
- 72 B. S. Murray, E. J. New, R. Pal and D. Parker, *Org. Biomol. Chem.*, 2008, **6**, 2085–2094.
- 73 S. J. Butler, M. Delbianco, L. Lamarque, B. K. McMahon, E. R. Neil, R. Pal, D. Parker, J. W. Walton and J. M. Zwieter, *Dalton Trans.*, 2015, **44**, 4791–4803.
- 74 M. Starck, R. Pal and D. Parker, *Chem. – Eur. J.*, 2016, **22**, 570–580.
- 75 S. J. Butler, B. K. McMahon, R. Pal, D. Parker and J. W. Walton, *Chem. – Eur. J.*, 2013, **19**, 9511–9517.
- 76 S. J. Butler, L. Lamarque, R. Pal and D. Parker, *Chem. Sci.*, 2014, **5**, 1750–1756.
- 77 J. W. Walton, A. Bourdolle, S. J. Butler, M. Soulie, M. Delbianco, B. K. McMahon, R. Pal, H. Puschmann, J. M. Zwieter, L. Lamarque, O. Maury, C. Andraud and D. Parker, *Chem. Commun.*, 2013, **49**, 1600–1602.
- 78 B. K. McMahon, R. Pal and D. Parker, *Chem. Commun.*, 2013, **49**, 5363–5365.
- 79 E. Pershagen, J. Nordholm and K. E. Borbas, *J. Am. Chem. Soc.*, 2012, **134**, 9832–9835.
- 80 H. Saneyoshi, Y. Ito and H. Abe, *J. Am. Chem. Soc.*, 2013, **135**, 13632–13635.
- 81 F. Kiehl, C. P. Montgomery, E. J. New, D. Parker, R. A. Poole, S. L. Richardson and P. A. Stenson, *Org. Biomol. Chem.*, 2007, **5**, 2975–2982.
- 82 C. G. Hartinger, M. Groessl, S. M. Meier, A. Casini and P. J. Dyson, *Chem. Soc. Rev.*, 2013, **42**, 6186–6199.
- 83 H. Simpkins, M. Figliomeni and M. Rosen, *Biochim. Biophys. Acta*, 1988, **972**, 25–32.
- 84 K. C. Fernando and G. J. Barritt, *Biochim. Biophys. Acta*, 1995, **1268**, 97–106.
- 85 P. R. Flatt, P. O. Berggren, E. Gylfe and B. Hellman, *Endocrinology*, 1980, **107**, 1007–1013.
- 86 J. Sneddon, *Biochem. Pharmacol.*, 1987, **36**, 3723–3730.
- 87 D. Bingham and M. Dobrota, *Biometals*, 1994, **7**, 142–148.
- 88 S. J. P. Damment and M. Pennick, *Clin. Pharmacokinet.*, 2008, **47**, 553–563.
- 89 Y. Cheng, Q. Huo, J. Lu, R. Li and K. Wang, *J. Biol. Inorg. Chem.*, 1999, **4**, 447–456.
- 90 P. Zimniak and E. M. Barnes, Jr., *J. Biol. Chem.*, 1980, **255**, 10140–10143.
- 91 M. Delbianco, V. Sadovnikova, E. Bourrier, G. Mathis, L. Lamarque, J. M. Zwieter and D. Parker, *Angew. Chem., Int. Ed.*, 2014, **53**, 10718–10722.
- 92 S. Gottschalk, J. Engelmann, G. A. Rolla, M. Botta, D. Parker and A. Mishra, *Org. Biomol. Chem.*, 2013, **11**, 6131.
- 93 X. Ai, L. Lyu, Y. Zhang, Y. Tang, J. Mu, F. Liu, Y. Zhou, Z. Zuo, G. Liu and B. Xing, *Angew. Chem., Int. Ed.*, 2017, **56**, 3031–3035.
- 94 N. S. Hwan, B. Y. Mi, P. Y. Il, K. J. Hyun, K. H. Min, C. J. Sig, L. K. Taek, H. Taeghwan and S. Y. Doug, *Angew. Chem., Int. Ed.*, 2011, **50**, 6093–6097.
- 95 Q. Zheng, H. Dai, M. E. Merritt, C. Malloy, C. Y. Pan and W.-H. Li, *J. Am. Chem. Soc.*, 2005, **127**, 16178–16188.
- 96 Z. Du, G. N. Borlace, R. D. Brooks, R. N. Butler, D. A. Brooks and S. E. Plush, *Inorg. Chim. Acta*, 2014, **410**, 11–19.
- 97 S. Quici, A. Casoni, F. Foschi, L. Armelao, G. Bottaro, R. Seraglia, C. Bolzati, N. Salvatore, D. Carpanese and A. Rosato, *J. Med. Chem.*, 2015, **58**, 2003–2014.
- 98 Z. Du, J. Sun, C. A. Bader, D. A. Brooks, M. Li, X. Li and S. E. Plush, *J. Inorg. Biochem.*, 2018, **178**, 32–42.
- 99 R. G. Anderson, B. A. Kamen, K. G. Rothberg and S. W. Lacey, *Science*, 1992, **255**, 410–411.
- 100 P. D. Prasad, V. B. Mahesh, F. H. Leibach and V. Ganapathy, *Biochim. Biophys. Acta*, 1994, **1222**, 309–314.
- 101 B. A. Kamen, A. K. Smith and R. G. Anderson, *J. Clin. Invest.*, 1991, **87**, 1442–1449.
- 102 K. H. Dixon, T. Mulligan, K. N. Chung, P. C. Elwood and K. H. Cowan, *J. Biol. Chem.*, 1992, **267**, 24140–24147.
- 103 G. R. Westerhof, G. Jansen, N. V. Emmerik, I. Kathmann, G. Rijkse, A. L. Jackman and J. H. Schornagel, *Cancer Res.*, 1991, **51**, 5507–5513.
- 104 G. R. Westerhof, J. H. Schornagel, I. Kathmann, A. L. Jackman, A. Rosowsky, R. A. Forsch, J. B. Hynes, F. T. Boyle, G. J. Peters and H. M. Pinedo, *Mol. Pharmacol.*, 1995, **48**, 459–471.
- 105 T. L. Kalber, N. Kamaly, P.-W. So, J. A. Pugh, J. Bunch, C. W. McLeod, M. R. Jorgensen, A. D. Miller and J. D. Bell, *Mol. Imaging Biol.*, 2011, **13**, 653–662.
- 106 S. Miotto, M. Bagnoli, F. Ottone, A. Tomassetti, M. I. Colnaghi and S. Canevari, *J. Cell. Biochem.*, 1997, **65**, 479–491.



- 107 R. A. Medina and G. I. Owen, *Biol. Res.*, 2002, **35**, 9–26.
- 108 W. H.-T. Law, L. C.-C. Lee, M.-W. Louie, H.-W. Liu, T. W.-H. Ang and K. K.-W. Lo, *Inorg. Chem.*, 2013, **52**, 13029–13041.
- 109 M. M. Alauddin, A. Y. Louie, A. Shahinian, T. J. Meade and P. S. Conti, *Nucl. Med. Biol.*, 2003, **30**, 261–265.
- 110 M. I. M. Prata, A. C. Santos, S. Torres, J. P. André, J. A. Martins, M. Neves, M. L. García-Martín, T. B. Rodrigues, P. López-Larrubia, S. Cerdán and C. F. G. C. Geraldies, *Contrast Media Mol. Imaging*, 2006, **1**, 246–258.
- 111 T. R. Townsend, G. Moyle-Heyrman, P. A. Sukerkar, K. W. MacRenaris, J. E. Burdette and T. J. Meade, *Bioconjugate Chem.*, 2014, **25**, 1428–1437.
- 112 M. J. Allen, K. W. MacRenaris, P. N. Venkatasubramanian and T. J. Meade, *Chem. Biol.*, 2004, **11**, 301–307.
- 113 J. Lee, M. J. Zylka, D. J. Anderson, J. E. Burdette, T. K. Woodruff and T. J. Meade, *J. Am. Chem. Soc.*, 2005, **127**, 13164–13166.
- 114 P. A. Sukerkar, K. W. MacRenaris, T. R. Townsend, R. A. Ahmed, J. E. Burdette and T. J. Meade, *Bioconjugate Chem.*, 2011, **22**, 2304–2316.
- 115 J. Lee, J. E. Burdette, K. W. MacRenaris, D. Mustafi, T. K. Woodruff and T. J. Meade, *Chem. Biol.*, 2007, **14**, 824–834.
- 116 W. B. Kauffman, T. Fuselier, J. He and W. C. Wimley, *Trends Biochem. Sci.*, 2015, **40**, 749–764.
- 117 S. Mohandessi, M. Rajendran, D. Magda and L. W. Miller, *Chem. – Eur. J.*, 2012, **18**, 10825–10829.
- 118 R. Brock, *Bioconjugate Chem.*, 2014, **25**, 863–868.
- 119 A. Walrant, S. Cardon, F. Burlina and S. Sagan, *Acc. Chem. Res.*, 2017, **50**, 2968–2975.
- 120 S. Heckl and U. Vogel, *J. Pharmacol. Exp. Ther.*, 2006, **319**, 657–662.
- 121 S. Heckl, J. Debus, J. Jenne, R. Pipkorn, W. Waldeck, H. Spring, R. Rastert, C. W. V. D. Lieth and K. Braun, *Cancer Res.*, 2002, **62**, 7018–7024.
- 122 K. L. Horton, K. M. Stewart, S. B. Fonseca, Q. Guo and S. O. Kelley, *Chem. Biol.*, 2008, **15**, 375–382.
- 123 A. Martin, A. Byrne, C. S. Burke, R. J. Forster and T. E. Keyes, *J. Am. Chem. Soc.*, 2014, **136**, 15300–15309.
- 124 J. Fernández-Carneado, M. Van Gool, V. Martos, S. Castel, P. Prados, J. de Mendoza and E. Giralt, *J. Am. Chem. Soc.*, 2005, **127**, 869–874.
- 125 J. Faiz Kayyem, R. M. Kumar, S. E. Fraser and T. J. Meade, *Chem. Biol.*, 1995, **2**, 615–620.
- 126 M. Shabnam, R. Megha, M. Darren and L. W. Miller, *Chem. – Eur. J.*, 2012, **18**, 10825–10829.
- 127 P. J. Endres, K. W. MacRenaris, S. Vogt and T. J. Meade, *Bioconjugate Chem.*, 2008, **19**, 2049–2059.
- 128 A. M. Prantner, V. Sharma, J. R. Garbow and D. Piwnica-Worms, *Mol. Imaging*, 2003, **2**, 15353500200303106.
- 129 I. I. Kruman, A. Nath and M. P. Mattson, *Exp. Neurol.*, 1998, **154**, 276–288.
- 130 M. Minnicozzi, M. A. M. Ramírez, R. W. Egan, G. J. Gleich, I. Kobayashi, D. Kim and W. N. Durán, *Microvasc. Res.*, 1995, **50**, 56–70.
- 131 K. L. Horton, M. P. Pereira, K. M. Stewart, S. B. Fonseca and S. O. Kelley, *ChemBioChem*, 2012, **13**, 476–485.
- 132 R. Bhorade, R. Weissleder, T. Nakakoshi, A. Moore and C.-H. Tung, *Bioconjugate Chem.*, 2000, **11**, 301–305.
- 133 R. Mishra, W. Su, R. Pohmann, J. Pfeuffer, M. G. Sauer, K. Ugurbil and J. Engelmann, *Bioconjugate Chem.*, 2009, **20**, 1860–1868.
- 134 M. Sibrian-Vazquez, J. Ortiz, I. V. Nesterova, F. Fernández-Lázaro, A. Sastre-Santos, S. A. Soper and M. G. H. Vicente, *Bioconjugate Chem.*, 2007, **18**, 410–420.
- 135 V. Polyakov, V. Sharma, J. L. Dahlheimer, C. M. Pica, G. D. Luker and D. Piwnica-Worms, *Bioconjugate Chem.*, 2000, **11**, 762–771.
- 136 S. I. Kirin, I. Ott, R. Gust, W. Mier, T. Weyhermüller and N. Metzler-Nolte, *Angew. Chem., Int. Ed.*, 2008, **47**, 955–959.
- 137 P. Haeffliger, N. Agorastos, A. Renard, G. Giambonini-Brugnoli, C. Marty and R. Alberto, *Bioconjugate Chem.*, 2005, **16**, 582–587.
- 138 F. Noor, A. Wüstholtz, R. Kinscherf and N. Metzler-Nolte, *Angew. Chem., Int. Ed.*, 2005, **44**, 2429–2432.
- 139 X. Zou, M. Rajendran, D. Magda and L. W. Miller, *Bioconjugate Chem.*, 2015, **26**, 460–465.
- 140 M. J. Allen and T. J. Meade, *J. Biol. Inorg. Chem.*, 2003, **8**, 746–750.
- 141 C. A. Puckett and J. K. Barton, *J. Am. Chem. Soc.*, 2009, **131**, 8738–8739.
- 142 P. Horcajada, R. Gref, T. Baati, P. K. Allan, G. Maurin, P. Couvreur, G. Férey, R. E. Morris and C. Serre, *Chem. Rev.*, 2012, **112**, 1232–1268.
- 143 A. Foucault-Collet, K. A. Gogick, K. A. White, S. Villette, A. Pallier, G. Collet, C. Kieda, T. Li, S. J. Geib, N. L. Rosi and S. Petoud, *Proc. Natl. Acad. Sci. U. S. A.*, 2013, **110**, 17199–17204.
- 144 C. Orellana-Tavra, S. A. Mercado and D. Fairen-Jimenez, *Adv. Healthcare Mater.*, 2016, **5**, 2261–2270.
- 145 C. Orellana-Tavra, S. Haddad, R. J. Marshall, I. Abánades Lázaro, G. Boix, I. Imaz, D. Maspoch, R. S. Forgan and D. Fairen-Jimenez, *ACS Appl. Mater. Interfaces*, 2017, **9**, 35516–35525.
- 146 K. A. White, D. A. Chengelis, M. Zeller, S. J. Geib, J. Szakos, S. Petoud and N. L. Rosi, *Chem. Commun.*, 2009, 4506–4508.
- 147 G. Mezei, C. M. Zaleski and V. L. Pecoraro, *Chem. Rev.*, 2007, **107**, 4933–5003.
- 148 T. N. Nguyen, C. Y. Chow, S. V. Eliseeva, E. R. Trivedi, J. W. Kampf, I. Martinic, S. Petoud and V. L. Pecoraro, *Chem. – Eur. J.*, 2018, **24**, 1031–1035.
- 149 J. C. Lutter, C. M. Zaleski and V. L. Pecoraro, in *Advances in Inorganic Chemistry*, ed. R. van Eldik and R. Puchta, Academic Press, 2018, vol. 71, pp. 177–246.
- 150 E. R. Trivedi, S. V. Eliseeva, J. Jankolovits, M. M. Olmstead, S. Petoud and V. L. Pecoraro, *J. Am. Chem. Soc.*, 2014, **136**, 1526–1534.
- 151 A. Krishan, *J. Cell Biol.*, 1975, **66**, 188–193.
- 152 I. Martinic, S. V. Eliseeva and S. Petoud, *J. Lumin.*, 2017, **189**, 19–43.
- 153 I. Martinic, S. V. Eliseeva, T. N. Nguyen, F. Foucher, D. Gosset, F. Westall, V. L. Pecoraro and S. Petoud, *Chem. Sci.*, 2017, **8**, 6042–6050.
- 154 B. Klajnert and M. Bryszewska, *Acta Biochim. Pol.*, 2001, **48**, 9.
- 155 D. Astruc, E. Boisselier and C. Ornelas, *Chem. Rev.*, 2010, **110**, 1857–1959.
- 156 Z. S. Pillai, P. Ceroni, M. Kubeil, J.-M. Heldt, H. Stephan and G. Bergamini, *Chem. – Asian J.*, 2013, **8**, 771–777.
- 157 A. Foucault-Collet, C. M. Shade, I. Nazarenko, S. Petoud and S. V. Eliseeva, *Angew. Chem., Int. Ed.*, 2014, **53**, 2927–2930.
- 158 J. H. S. K. Monteiro, D. Machado, L. M. de Hollanda, M. Lancellotti, F. A. Sigoli and A. de Bettencourt-Dias, *Chem. Commun.*, 2017, **53**, 11818–11821.
- 159 V. V. Utochnikova, D. S. Koshelev, A. V. Medvedko, A. S. Kalyakina, I. S. Bushmarinov, A. Y. Grishko, U. Schepers, S. Bräse and S. Z. Vatsadze, *Opt. Mater.*, 2017, **74**, 191–196.
- 160 N.-D. H. Gamage, Y. Mei, J. Garcia and M. J. Allen, *Angew. Chem., Int. Ed.*, 2010, **49**, 8923–8925.

